Measurement of Macrophage Adhesion at Various pH Values by Optical Tweezers with Backward-Scattered Detection

2010 Jpn. J. Appl. Phys. 49 077002

(http://iopscience.iop.org/1347-4065/49/7R/077002)

Measurement of Macrophage Adhesion at Various pH Values by Optical Tweezers with Backward-Scattered Detection

Yi-Jr Su* and Long Hsu

Institute and Department of Electrophysics, National Chiao-Tung University, 1001 Ta Hsueh Road, Hsinchu, Taiwan 30010, R.O.C.

Received January 15, 2010; revised March 26, 2010; accepted April 8, 2010; published online July 20, 2010

Optical tweezers have emerged as a powerful tool with broad applications in biology and physics. In force-measuring applications, the trapped bead position is usually accurately determined by forward-scattered detection. The current study discusses both backward-scattered detection and forward-scattered detection related to the linear detection range for a 3 μm bead and the distance between the two laser system focuses, confirming the optimum positions of the two focuses. The result indicates that the linear detection range of backward-scattered detection is longer than the forward-scattered one. Finally, this work investigates real-time adhesion force measurements between human macrophages and 3 μm trapped beads coated with lipopolysaccharides at various pH values by optical tweezers with backward-scattered detection.

DOI: 10.1143/JJAP.49.077002

1. Introduction

Macrophages are members of the leukocyte family. Leukocytes normally circulate in the blood stream by deforming passively to minimize disturbances to the environment. Tissue damage causes inflammation and release of vasoactive and chemotactic factors, which trigger a local increase in blood flow and capillary permeability. Then, leukocytes accumulate quickly to the infection site. The leukocyte extravasation process takes place according to a sequence of events that involve tethering, activation by a chemoattractant stimulus, adhesion by integrin binding, and migrating to the infection site. To accomplish this, leukocytes must recognize the inflamed endothelium and adhere strongly enough so that they are not swept away by flowing blood.[1)] Macrophages are activated by a variety of stimuli in the course of an immune response and excel at phagocytosis. Phagocytosis plays an important role in host defense against invading pathogens. In this receptor-mediated process, large particles like bacteria or yeast are ingested by the plasma membrane of macrophages. The phagocytosis process can be divided into four discrete steps: adhesion, ingestion, fusion with lysosomes, and degradation.[2)] The leukocyte extravasation process and macrophage phagocytosis reveal that adhesion is an important part of the immune system.

Over the past three decades, researches have extensively investigated the mechanics of cellular adhesion, which are the important objects in biophysics. Earlier methods for evaluating adhesive force include counting the number of bound cells in a parallel plate under shear flow conditions,[3)] using micropipette suction,[4)] an atomic force microscope (AFM) or optical tweezers to measure the adhesive force of a single live cell.[5,6)] The counting method of bounded cells provides a simple and convenient approach to describe adhesive force but cannot reveal real-time dynamic information. The micropipette suction method directly uses spherical cells or beads as force transducers to measure adhesive forces of a single live cell but it is difficult to control stationary pressure inside a micropipette. Studies have used AFM to determine mechanical properties and for determining molecule–molecule and receptor–ligand interactions,[7)] as it is the most versatile instrument. However, the tip of a cantilever usually stabs the cell while measuring the adhesive force by AFM.

Optical tweezers has become an important tool to measure forces in biology. The near infrared light is typically used as a laser source to reduce the damage to a cell or cellular organelles and the biological objects can be held and moved by exerting piconewton (pN) forces. The system has many applications such as force measurements of molecular motors or macro-molecules, imaging three-dimensional cavity structures, and studying small variations in local diffusion or viscosity. Optical tweezers perform a wider range of experiments through the integration of a quadrant photodiode (QPD) for position detection.[8–11)] Both forward-scattered detection and backward-scattered detection are the typical position detection. Forward-scattered detection accurately describes the position of the trapped particle to the trap center by measuring the deflection of the transmitted laser light. The trapped particle, driven by Brownian motion, is in a harmonic potential built by the optical tweezers. Generally, these trapped particle signals from the position detection system are applied to calibrate stiffness of the optical tweezers by mean square displacement method[12)] or power spectrum method.[12–15)] The power spectrum method not only gets the trapping stiffness but simultaneously provides the viscosity to help us to monitor the environmental variations, although the mean square displacement method is simpler than power spectrum method. In force measurement, adhesive force strength is calculated by multiplying trapping stiffness and trapped bead displacement. The optical tweezers probe is a spherical particle that can avoid the AFM disadvantage to not hurt the cell.

However, in forward-scattered detection, the cellular environment affects the transmitted laser light when measuring individual bond strength by attaching and detaching optically trapped particles to immobilized cells.[16)] The transmitted laser light is the interference between forward-scattered light from the bead and unscattered light. Many kinds of suspensions from a cellular medium influence the interference when the transmitted laser light passes through the cellular environment. Backward-scattered detection effectively reduces the cellular environment influence because the objective directly collects backward-scattered light without passing through the cellular environment. Furthermore, the setup of backward-scattered detection no

*E-mail address: pkids.ep90g@nctu.edu.tw

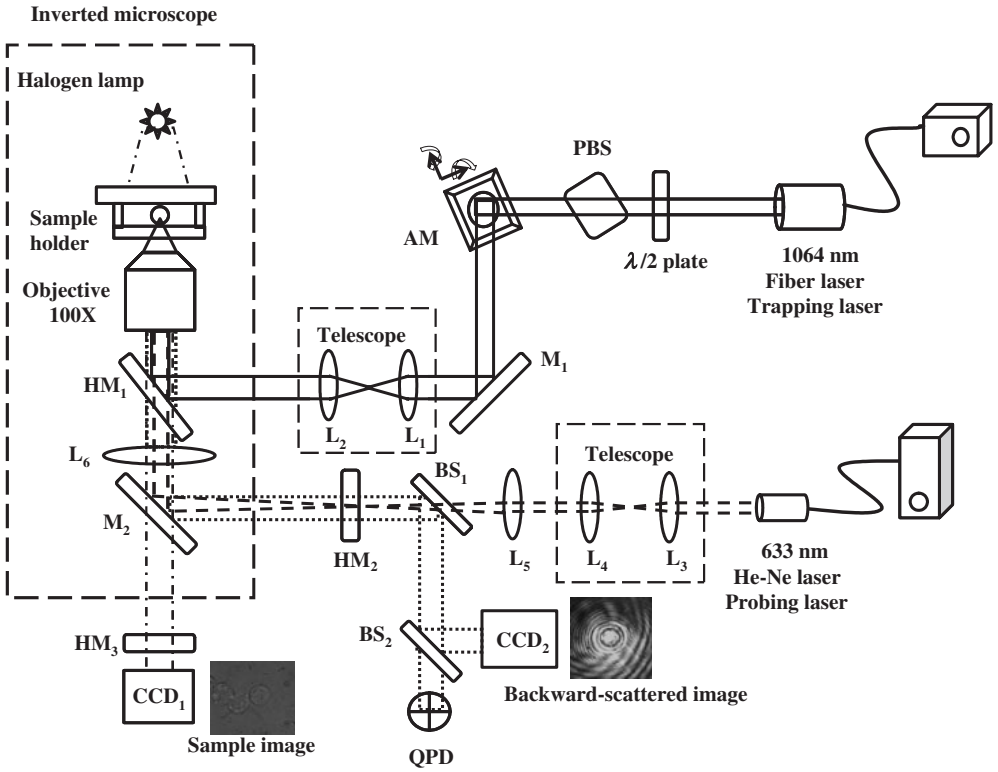

Fig. 1. Schematic diagram of the optical tweezers system with backward-scattered detection. Experimental setup: PBS: polarization beamsplitter cube, AM: gimbal-mounted mirror driven with piezo actuators, M: reflective mirror, L: lens, HM: hot mirror, BS: beamsplitter, QPD: quadrant photodiode, and CCD: charge coupled device camera.

longer requires a condenser, making it possible to combine the PFM with other techniques such as the AFM.

This paper only considers the force in the lateral direction because force measurement in one dimension is sufficient for most single molecule detaching experiments.[16] Some literatures mention using backward-scattered light as a signal for force detection, but only discuss backward-scattered light due to the optical tweezers without the probing beam system.[17] The current study discusses both backward-scattered detection and forward-scattered detection that add a probing beam and their linear detection ranges that describe the precise position of the trapped bead. Lipopolysaccharides (LPS), a major component of the outer membrane of bacteria, act an endotoxin and induce a strong response from normal animal immune systems. Finally, this work investigates real-time adhesion force measurements of the interaction between human macrophages and micro-sized beads coated with LPS at various pH values using optical tweezers with backward-scattered detection.

2. Materials and Methods

2.1 Experimental setup

Figure 1 shows the experimental setup of our optical tweezers with backward-scattered detection. A fiber laser (IPG Photonics YLR-10-1064, 1064 nm) was used as a light source for the trapping laser. The laser was reflected by a hot mirror (HM_1) and its diameter overfilled the back aperture of the objective. A half-wave plate and a polarizing beam splitter cube were integrated to control the laser power. A reflective mirror driven with piezoelectric actuators (New Focus 8807) reflected the trapping laser and moved the optical trap along the horizontal plane. A telescope, typically in a 1 : 1 configuration, was used to keep the trapping power constant in the specimen plane. Because the reflective mirror and the back aperture of the objective, optically conjugate to each other, have the same diameter of the trapping laser regardless of the laser movement. Changing the telescope spacing also changes the laser divergence that enters the objective, and the axial location of the laser focus. The experiment steered the laser beam into a modified inverted microscope (Nikon TE2000-U) and the high numerical aperture (NA) oil-immersion objective (Nikon Plan Apo VC, 100×, NA = 1.4) yielded a tight focus to trap micro-sized beads. The maximum power of the trapping laser at the back aperture of the objective was 800 mW.

This study also used the probing laser (LASOS Lasertechnik LGK 7628, 632.8 nm, He-Ne Laser) to detect the position of a trapped micro-sized bead. A telescope with micrometer position adjustment steered the focal spot of the detection beam. The laser passed through a beam splitter and then moved into the microscope via the side port. The high NA objective simultaneously collected the backward-scattered light of the probing laser from the trapped bead, and the light was imaged on a quadrant photodiode (QPD; Hamamatsu G6849) through a hot mirror (HM_2) and a beam splitter (BS_1). A second beam splitter (BS_2) in the detection path was used to observe the backward-scattered pattern with a charge coupled device camera (CCD_1).

The QPD was mounted on a dual-axis translation stage to move the QPD position so that the backward-scattered pattern could be projected on the center of the detector. The QPD converted the power of incident light to four voltages to monitor the position of the trapped micro-sized bead. The voltage difference in each direction was converted to an

intensity independent position signal. The voltage signal outputs from the QPD were processed by a preamplifier and then by a main amplifier (MSR-Technik Öffner) with a maximum amplification factor of 500 and a cut-off frequency of 1 MHz. Voltage signals of the four channels were simultaneously recorded by a data acquisition card with a sampling rate of up to 10 MHz. A bright-field illumination was achieved using a halogen lamp through a condenser. The images were taken using a charge coupled device camera (CCD_2) with a hot mirror (HM_3) blocking infrared light. In this experiment, the x–y position of the sample was controlled precisely based on the piezo-electrical controlled sample holder.

2.2 Force calibration

The trapping force due to optical tweezers was calculated by multiplying trapping stiffness and displacement of a trapped bead. The experiment used the power spectrum density (PSD) method, based on thermal fluctuations of the trapped bead, to estimate trapping stiffness. The Brownian motion of a trapped bead near the center of the optical tweezers in one dimension is well described by the Langevin equation:[13)]

$$\gamma \frac{dx(t)}{dt} + k_{\mathrm{OT}} x(t) = F(t), \tag{1}$$

where $F(t)$ is the random thermal force, k_{OT} is the trapping stiffness, and $\gamma = 6\pi\eta a$ denotes the Stokes drag coefficient for a micro-sized bead of radius a moving in a fluid with viscosity η. The PSD of the trapped bead is described by a Lorentzian function:

$$S_x(f) = \frac{k_{\mathrm{B}}T}{\gamma\pi^2(f_{\mathrm{c}}^2 + f^2)}, \tag{2}$$

where k_{B} is Boltzmann's constant, T is the absolute temperature, and

$$f_{\mathrm{c}} = \frac{k_{\mathrm{OT}}}{2\pi\gamma} \tag{3}$$

is the corner frequency. The PSD of the thermal force, $F(t)$, is given by $S_{\mathrm{F}}(f) = 4\gamma k_{\mathrm{B}}T$. The corner frequency divides the Brownian motion into two regions. When $f \gg f_{\mathrm{c}}$, the PSD drops as $1/f^2$, indicating free diffusion. When $f \ll f_{\mathrm{c}}$, the PSD is approximately constant, given by

$$S_x(0) \approx \frac{k_{\mathrm{B}}T}{\gamma\pi^2 f_{\mathrm{c}}^2} = \frac{4\gamma k_{\mathrm{B}}T}{k_{\mathrm{OT}}^2}. \tag{4}$$

In the position calibration, the trapped bead of 3 μm diameter was moved by tilting the gimbal-mounted mirror to pass through the focus of the probing laser. The inset of Fig. 2 describes the relations between the detector responses and the trapped particle positions. This inset provides a detector sensitivity of 0.394 V/μm and a linear detection range of the trapped bead of 1.97 μm. Figure 2 shows the PSD of a 3 μm bead in the culture medium, as shown by the black line. The PSD was fitted to a Lorentzian function, as shown by the dash line. This measurement yielded a corner frequency of 1070 Hz and a trap stiffness of 190 pN/μm.

2.3 Cell culture

Macrophages (American Type Culture Collection ATCC No. TIB-202, cell line Thp-1) were cultured under standard procedures for use in the adhesion experiments. The cells were maintained in RPMI 1640 medium (Gibco) supplemented with 10% FBS, L-glutamine, and penicillin at 37 °C in 5% CO_2-humidified incubators. The cells were suspended in the cell culture medium at a final concentration of 5×10^5 cells/ml. Differentiation and adherence were obtained by incubation with phorbol 12-myristate 13-acetate (PMA; Sigma Aldrich 100–160 nM) for 1–3 days.[18)] Before experiments, the cells were washed off the culture dish with phosphate-buffered saline (PBS) and maintained in RPMI 1640 medium containing 10% FBS for 30 min.

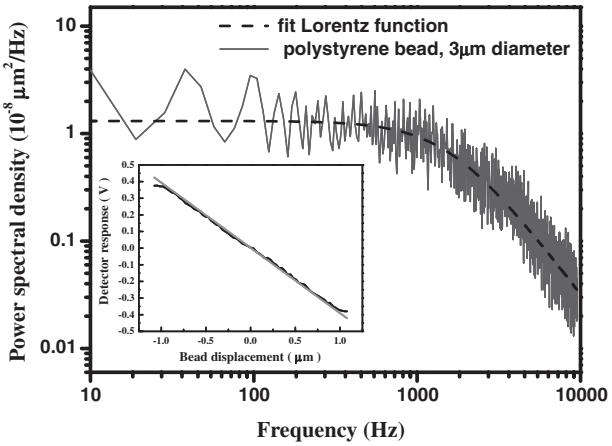

Fig. 2. Power spectral density of the thermal position fluctuations of a 3 μm bead in the laser trap (solid line). The fit of a Lorentz function to determine the corner frequency and the trapping stiffness (dash line). The inset shows the position calibration of the quadrant photodetector. The detector responses to the trapped bead displacements are described in the black line and their fitting line described by the gray line.

2.4 Preparation of LPS-coated beads

Adsorption of LPS onto polystyrene micro-sized beads was based on an early paper of Ofek *et al.*[19)] Equal volumes of polystyrene micro-sized beads (3 μm diameter, Molecular Probes) were mixed with LPS (200 mg/ml) in PBS. The mixture was incubated for 4 h at room temperature and the micro-sized beads were then blocked with LPS. After blocking, the micro-sized beads were washed and centrifuged at 7,000 rpm for 5 min in a microcentrifuge. The procedure was repeated twice to remove nonadsorbed LPS.

3. Results and Discussion

Figure 3 is used to discuss backward- and forward-scattered detections by the position calibration of a 3 μm bead. The backward-scattered patterns were recorded for the three bead displacements −1.2, 0.0, and 1.2 μm, respectively, indicated in the deflection curve with a, b, and c, in the top of Fig. 3(a). The patterns not only shifted with different displacements, but also changed their shape when the optical tweezers moved the trapped bead. By the position calibration, the detector responses to the trapped bead displacements are described in the black line and their fitting line is described by the gray line, in the middle of Fig. 3(a). To precisely describe the position of the trapped bead, it is necessary to define a linear detection range where the trapped bead displacement is proportional to detector

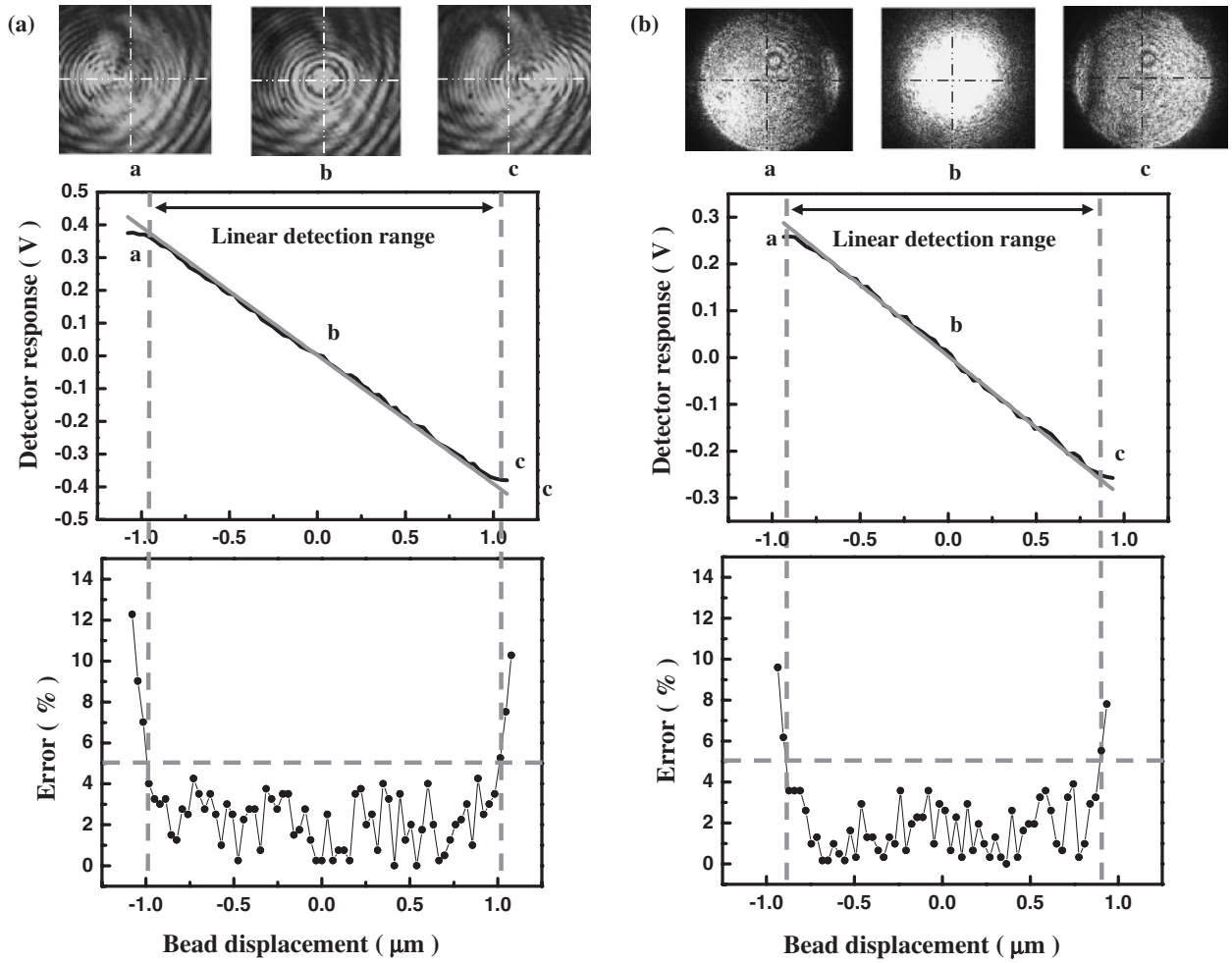

Fig. 3. Comparison between (a) backward-scattered detection and (b) forward-scattered detection. The top of figure shows their scattered patterns, recorded at a bead position of a, b, and c. These positions are also indicated in the deflection curves of the middle of figure. The detector responses to the trapped bead displacements are described in the black line and their fitting lines are described by the gray line. The bottom of figure uses to determine the linear detection range where the deviation was less than 5%.

response. The bottom of Fig. 3(a) shows the difference between the detector response and the fitting line, divided by the magnitude of the fitting line at 1.0 μm, represented an error percentage. We determined the linear detection range where the deviation was less than 5%,[17] and the linear detection range of the 3.0 μm bead was 1.97 μm in backward-scattered detection.

Both forward-scattered detection and backward-scattered detection have the same trapping setup. A condenser lens with a NA of 0.4 was added on the upper side of the sample holder to collect forward-scattered light in forward-scattered detection. The QPD was placed behind the conjugate back focal plane of the condenser lens. A beam splitter was placed in between the condenser lens and the QPD and 50% of the transmitted light on a CCD camera for observing the forward-scattered pattern. A dichroic mirror in front of this beam splitter was used to reflect the transmitted light and allow the invisible infrared light to pass. The top of Fig. 3(b) records the forward-scattered patterns from the three bead displacements −1.1, 0.0, and 1.1 μm and respectively indicates the deflection curve with a, b, and c. These patterns differ from backward-scattered patterns and also describe the bead's position by interference variation. In the middle of Fig. 3(b), the black line and gray line also describe the forward-scattered detector responses and their fitting line. Under the same method discussed above, the linear detection range of the 3.0 μm bead was 1.74 μm, in the bottom of Fig. 3(b).

Figure 4(a) indicates the linear detection ranges of these two detections with the vertical differences, z_d, and z_d used to describe the vertical difference of two focuses between the probing laser and the trapping laser, as shown in Fig. 4(b). The linear detection range of backward-scattered detection is labeled with a solid square and forward-scattered detection is labeled with a solid circle. We fixed the axial location of the focus of the trapping laser in the experiment and then z_d depended on the telescope spacing that the probing laser passed through. The relation between the telescope spacing and z_d roughly determined by ray tracing[20] in the probing beam system. Furthermore, the sample stage was finely tuned to confirm the position of the focus of the probing laser by tracing the image of the laser focus. Figure 4(a) shows that both backward- and forward-scattered detections have a maximum linear detection range. The maximum linear detection range of backward-scattered light is 1.97 μm at $z_d = 2$ μm and forward scattered light is 1.74 μm at $z_d = -2$ μm. The two focus positions of the probing laser, symmetrically focused on the trapping laser, provide maximum linear

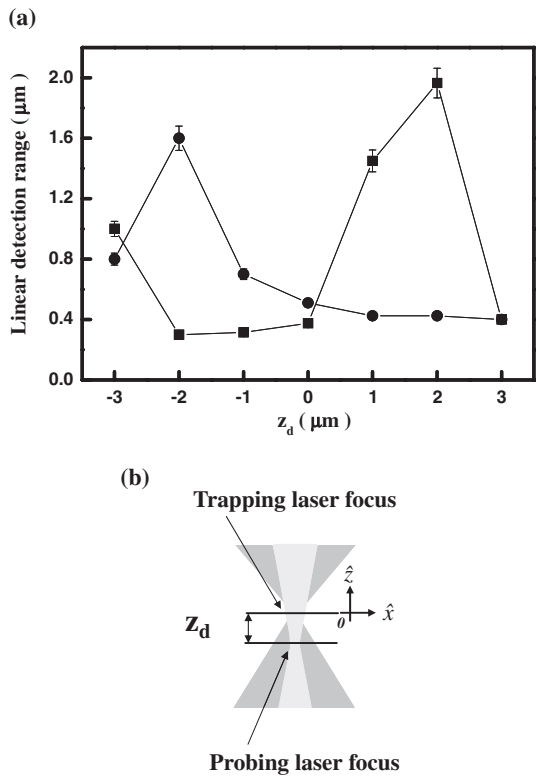

Fig. 4. (a) Comparison of the linear detection range between backward-scattered detection (solid square) and forward-scattered detection (solid circle). (b) The definition of z_d.

detection ranges. The maximum of backward-scattered detection is longer than the forward-scattered one. Hence, backward-scattered detection measures the longer displacement of the trapped bead in adhesive force measurement.

As discussed above, macrophage adhesion with LPS was measured by optical tweezers with backward-scattered detection. Force measurement calculates trapping force by multiplying trapping stiffness of the optical tweezers and trapped bead displacement. As shown in Fig. 5(a), an immobilized macrophage is moved toward a trapped bead by the computer-controlled stage driven with piezoelectric actuator. Adhesive force is determined by attaching and detaching optically trapped beads to immobilized macrophages. Figure 5(b) describes a typical record of the bead's displacement during the measurement and position of the bead along with time that exhibits a triangle-like shape. Therefore, the peak of the triangle indicates when the trapping force is sufficient to detach the bead from the macrophage and obtain adhesive force. Figure 5(c) shows the macrophage and the trapped bead coated with LPS during an actual adhesion experiment. Figure 5(d) shows a representative AFM image of the trapped bead coated with LPS.

Figure 6 shows the real-time adhesion force measurement of increased contact area. The experiment increased applied force to push the trapped bead to increase contact area with a macrophage. Then, optical tweezers detached the trapped bead from the macrophage to produce two bond ruptures. The strengths of two bonds were almost the same. The result indicates that increased contact area would not change the adhesive forces of individual bonds but could cause the formation of multiple bonds to raise total adhesive force. Similarly, increased contact time only raises total adhesive force.[21] To reduce multi-bond affection, the retraction speed of the stage was adjusted to 1 μm/s and the contact time between attaching and detaching was kept at 0.4 s.[16] Macrophage activity is influenced by temperature but the adhesive forces change only very little between 23 and

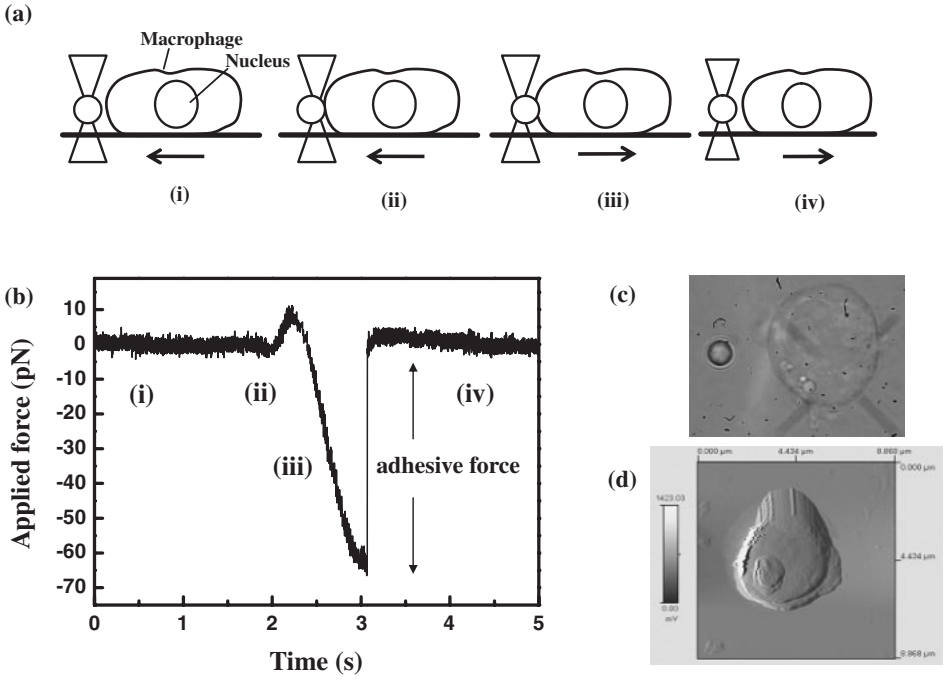

Fig. 5. A schematic presentation describing the different steps of the adhesive force measurement. (a-i) The trapped bead is under a confined Brownian motion. (ii) The bead contacts a macrophage by optical tweezers. (iii) The bead is pulled away from the trapping center. (iv) The trapping force is larger than the adhesive force so that the bead is detached from the macrophage and returned to its equilibrium position in the trap. (b) Force trace of an actual adhesion experiment. (c) An image during an actual adhesion experiment. (d) An AFM image of the trapped bead coated with LPS.

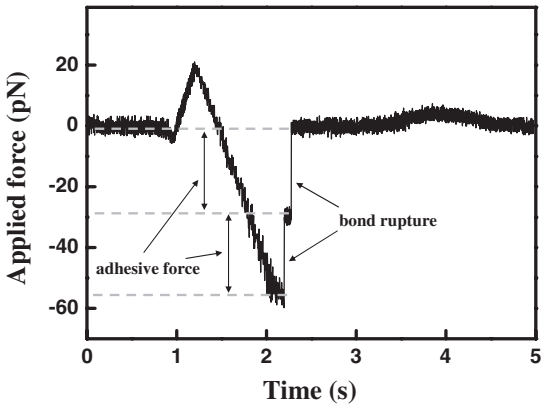

Fig. 6. Force trace of an actual adhesion experiment at pH 6. Increased contact area causes the formation of multiple bonds.

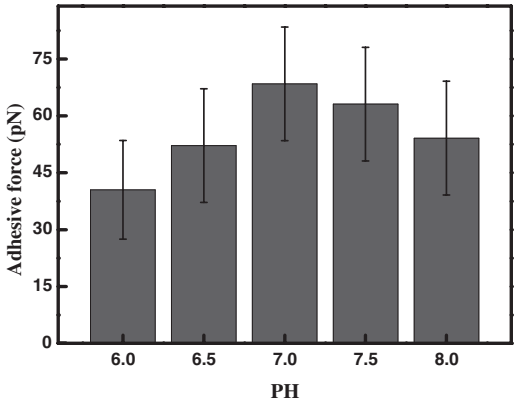

Fig. 8. The averages of the adhesive forces at various pH values.

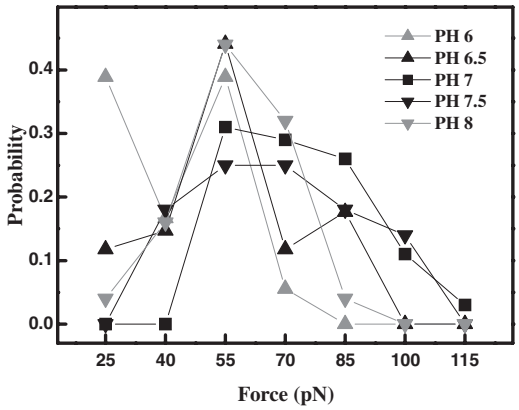

Fig. 7. The probability of successful macrophages–LPS adhesion events at various pH values.

37 °C.[16] All experiments were finished at room temperature and completed in 30 min. Using optical tweezers with backward-scattered detection, the adhesive forces between macrophages and LPS were 65.1 ± 5.3 pN at pH 7 and the forces between macrophages and polystyrene beads were 26.0 ± 1.1 pN at pH 7. In the report of Knöner's group,[16] mean adhesive forces between mouse macrophages and polystyrene beads were 20 pN measured by optical tweezers with forward-scattered detection. Although human macrophages and mouse macrophages are different, they have the same function in the immune system. The value of adhesive force from our detection is similar to Knöner's group.

The probability of successful macrophages–LPS adhesion events at various pH values are shown in Fig. 7. The adhesive forces are between 25 and 70 pN at pH 6, and the probability distribution has two peaks at 25 and 55 pN. At pH 6.5 and 8, the adhesive forces are between 55 and 85 pN and the probability distribution has one peak at 55 pN. The adhesive forces are between 55 and 115 pN at pH 7 and the probability distribution decreases with adhesive force. The adhesive forces are between 40 and 100 pN at pH 7.5 and the probability distribution approached a Gaussian-like appearance. From pH 6 to 8, the adhesive force of 55 pN has the maximum probability in each pH group. It indicates that culture medium pH does not influence the binding strength of 55 pN between LPS and macrophages. The variations of adhesive force ranges at various pH values also indicate that some formations of receptor–ligand pairs between LPS and macrophages relate to a specific pH value. These results show clearly that many kinds of receptor–ligand pairs exist between LPS and macrophages. The averages of adhesive forces at various pH values are shown in Fig. 8. This figure describes that the average values of adhesive force has a maximum at pH 7. The strength of average adhesive force at pH 7.5 is close to the strength at pH 7. Culture medium pH at 7 and 7.5 enhances macrophage adhesion to help its phagocytosis to work effectively.

4. Conclusions

This study discusses both backward- and forward-scattered detections to find the longest distance linear detection range for a 3 μm bead. The result indicates that the linear detection range of backward-scattered detection is longer than the forward-scattered one. This study also discusses both detections related to the linear detection range and the distance between the two laser system focuses, confirming the optimum positions of the two focuses. As discussed above, backward-scattered detection provides the longer detection range, 1.97 μm, at $z_d = 2$ μm. Then, we examined the LPS coat of the 3 μm bead by AFM to make sure of macrophage adhesion with LPS. Finally, the adhesive forces between trapped beads coated with LPS and living macrophages at various pH values were investigated by optical tweezers with backward-scattered detection. We demonstrate that culture medium pH can affect the binding strength of receptor–ligand pairs between LPS and macrophages. But we also find that culture medium pH dose not influence the receptor–ligand pair of the adhesion strength of 55 pN. These results indicate that many kinds of receptor–ligand pairs exist between LPS and macrophages. Through data analysis, we verify that culture medium pH at 7 and 7.5 enhances macrophage adhesion and this result may indicate that immunity is more powerful in this range.

Acknowledgement

The authors would like to thank the National Science Council of the Republic of China, Taiwan, for financially supporting this research under Contract No. NSC98-2221-E-009-029.

1) T. J. Kindt, R. A. Goldsby, B. A. Osborne, and J. Kuby: in *Immunology*, ed. K. Ahr (Freeman, New York, 2007) p. 332.
2) T. D. Pollard and W. C. Earnshaw: in *Cell Biology*, ed. W. R. Schmitt (Saunders, Philadelphia, PA, 2002) p. 356.
3) J. J. Chiu, C. N. Chen, P. L. Lee, C. T. Yang, H. S. Chuang, and S. Chien: J. Biomech. **36** (2003) 1883.
4) J. Shao and R. M. Hochmuth: Biophys. J. **71** (1996) 2892.
5) E. Canetta, A. Duperray, A. Leyrat, and C. Verdier: Biorheology **42** (2005) 321.
6) J. A. Berliner, D. K. Vora, and P. T. Shih: in *Vascular Adhesion Molecules and Inflammation*, ed. J. D. Pearson (Birkhäuser, Basel, 1999) p. 239.
7) F. Li, S. D. Redick, H. P. Erickson, and V. T. Moy: Biophys. J. **84** (2003) 1252.
8) K. Visscher and S. M. Block: Methods Enzymol. **298** (1998) 460.
9) K. Visscher, M. J. Schnitzer, and S. M. Block: Nature (London) **400** (1999) 184.
10) A. Rohrbach and E. H. K. Stelzer: J. Appl. Phys. **91** (2002) 5474.
11) J. K. Dreyer, K. Berg-Sørensen, and L. Oddershede: Appl. Opt. **43** (2004) 1991.
12) K. C. Neuman and S. M. Block: Rev. Sci. Instrum. **75** (2004) 2787.
13) K. Svoboda and S. M. Block: Annu. Rev. Biophys. Biomol. Struct. **23** (1994) 247.
14) M. W. Allersma, F. Gittes, M. J. deCastro, R. J. Stewart, and C. F. Schmidt: Biophys. J. **74** (1998) 1074.
15) K. Berg-Sørensen and H. Flyvbjerg: Rev. Sci. Instrum. **75** (2004) 594.
16) G. Knöner, B. E. Rolfe, J. H. Campbell, S. J. Parkin, N. R. Heckenberg, and H. Rubinsztein-Dunlop: Biophys. J. **91** (2006) 3085.
17) J. H. G. Huisstede, K. O. van der Werf, M. L. Bennink, and V. Subramaniam: Opt. Express **13** (2005) 1113.
18) S. V. D. Velde, H. A. Nguyen, F. V. Bambeke, P. M. Tulkens, J. Grellet, V. Dubois, C. Quentin, and M.-C. Saux: J. Antimicrob. Chemother. **62** (2008) 518.
19) I. Ofek, A. Mesika, M. Kalina, Y. Keisari, R. Podschun, H. Sahly, D. Chang, D. McGregor, and E. Crouch: Infect. Immun. **69** (2001) 24.
20) E. Fällman and O. Axner: Appl. Opt. **36** (1997) 2107.
21) E. B. Lomakina and R. E. Waugh: Biophys. J. **86** (2004) 1223.